communications biology

Article

https://doi.org/10.1038/s42003-024-06645-0

Acinetobacter baumannii OmpA-like porins: functional characterization of bacterial physiology, antibiotic-resistance, and virulence

Check for updates

Daniela Scribano[1,11], Elena Cheri[2,11], Arianna Pompilio[3,4], Giovanni Di Bonaventura[3,4], Manuel Belli[5,6], Mario Cristina[6,7], Luigi Sansone[5,6], Carlo Zagaglia[1], Meysam Sarshar[2], Anna Teresa Palamara[8,9] & Cecilia Ambrosi[5,10] ✉

Acinetobacter baumannii is a critical opportunistic pathogen associated with nosocomial infections. The high rates of antibiotic-resistance acquisition make most antibiotics ineffective. Thus, new medical countermeasures are urgently needed. Outer membrane proteins (OMPs) are prime candidates for developing novel drug targets and antibacterial strategies. However, there are substantial gaps in our knowledge of *A. baumannii* OMPs. This study reports the impact of OmpA-like protein on bacterial physiology and virulence in *A. baumannii* strain AB5075. We found that PsaB (ABUW_0505) negatively correlates to stress tolerance, while ArfA (ABUW_2730) significantly affects bacterial stiffness, cell shape, and cell envelope thickness. Furthermore, we expand our knowledge on YiaD (ABUW_3045), demonstrating structural and virulence roles of this porin, in addition to meropenem resistance. This study provides solid foundations for understanding how uncharacterized OMPs contribute to *A. baumannii*'s physiological and pathological processes, aiding the development of innovative therapeutic strategies against *A. baumannii* infections.

Acinetobacter baumannii is a Gram-negative opportunistic pathogen responsible for several serious infections, including pneumonia, sepsis, and meningitis, particularly in critically ill patients[1]. The increased number of infections caused by carbapenem- and colistin-resistant strains poses major therapeutic dilemmas[2]. The failure of the novel siderophore cephalosporin, cefiderocol, in treating infections caused by pan-drug-resistant *A. baumannii* strains showed how fast these bacteria develop adaptation mechanisms[3]. Consequently, *A. baumannii* is currently recognized as a menace to public health against which novel drug targets and antibacterial strategies must be developed (https://www.who.int/news/item/27-02-2017-who-publishes-list-of-bacteria-for-which-new-antibiotics-are-urgently-needed). In the last years, the outer membrane protein A (OmpA) was selected as a potential candidate for new drug and vaccine strategies[4–8]. As in other gram-negative bacteria, OmpA is the most abundant porin embedded within the outer membrane (OM) in *A. baumannii*. This protein comprises an N-terminal eight-stranded β-barrel that resides within the OM with four loops exposed in the extracellular milieu and a C-terminal periplasmic domain that binds the peptidoglycan and contributes to cell-envelope stability[9]. Besides its physiological roles as a small molecule channel, membrane-embedded OmpA is involved in resistance to antibiotics and serum, biofilm formation, and host interaction[9–16]. In addition, OmpA released via OM vesicles targets mitochondria in host cells, and it is responsible for mitochondrial fragmentation and apoptosis through the release of the pro-apoptotic molecule cytochrome C[17–20]. Accordingly, *ompA*

[1]Department of Public Health and Infectious Diseases, Sapienza University of Rome, Rome, Italy. [2]Research Laboratories, Bambino Gesù Children's Hospital, IRCCS, Rome, Italy. [3]Department of Medical, Oral and Biotechnological Sciences, "G. d'Annunzio" University of Chieti-Pescara, Chieti, Italy. [4]Center for Advanced Studies and Technology (CAST), "G. d'Annunzio" University of Chieti-Pescara, Chieti, Italy. [5]Department of Human Sciences and Quality of Life Promotion, San Raffaele University, Rome, Italy. [6]Laboratory of Molecular and Cellular Pathology, IRCCS San Raffaele Roma, Rome, Italy. [7]Department of Molecular Medicine, Sapienza University of Rome, Rome, Italy. [8]Department of Infectious Diseases, Istituto Superiore di Sanità, Rome, Italy. [9]Department of Public Health and Infectious Diseases, Sapienza University of Rome, Laboratory Affiliated to Institute Pasteur Italia-Cenci Bolognetti Foundation, Rome, Italy. [10]Laboratory of Microbiology of Chronic-Neurodegenerative Diseases, IRCCS San Raffaele Roma, Rome, Italy. [11]These authors contributed equally: Daniela Scribano, Elena Cheri.
✉e-mail: cecilia.ambrosi@uniroma5.it

mutants showed reduced growth rate, motility, serum resistance, adhesion to human A549 lung epithelial cells, and virulence in animal models[13,17]. Despite some variability in the external loops and the C-terminus, the amino acid sequence of OmpA showed an overall similarity among a considerable number of clinical *A. baumannii* isolates[21].

Other OMPs have been characterized so far. CarO was initially identified as the porin responsible for imipenem influx into *A. baumannii* cells[22], an OM channel with eight β-barrel structures involved in the passage of small molecules[23]. Up to now, six variants of CarO have been found within *A. baumannii* strains with different specificities to imipenem; interestingly, *carO* expression is fine-tuned post-transcriptionally by the master regulator Hfq to better adapt to the bacterial niche[24]. In addition, five different porins, OccAB1-5 (formerly OprD-like), have been found in *A. baumannii* clinical isolates[25], with OccAB1 (OprD) mainly involved in stress survival and in vivo virulence[26,27]. Initially associated with carbapenem resistance, porin Omp33–36, also known as Omp34, was shown to be critical for bacterial growth and in vitro and in vivo virulence in *A. baumannii*[28]. Recently, the OMP YiaD was characterized as an OmpA-like protein favoring the entrance of meropenem into *A. baumannii* cells[29]. Furthermore, it was shown that YiaD influences colony morphology as well as biofilm formation[29].

These findings indicated that bacterial OMPs are directly involved in mitigating and adapting to changing environmental conditions to maintain cell homeostasis; consequently, their characterization is paramount for preventing and treating *A. baumannii* infections. Therefore, this study aimed to elucidate the role of OmpA-like proteins of *A. baumannii* AB5075 in fitness, antibiotic resistance, stress response, and in vitro and in vivo virulence.

Results

Identification of genes encoding OmpA-like proteins and analysis of Tn26 mutants in AB5075

A manual search of the *A. baumannii* AB5075 complete genome (Accession number CP008706) (https://www.ncbi.nlm.nih.gov/nucleotide/CP008706) for *ompA*-like genes retrieved six genes, ABUW_0505 (*psaB*), ABUW_0649 (*ompA*), ABUW_1015 (*carO*), ABUW_2571 (*dotU1*), ABUW_2730 (*arfA*), and ABUW_3045 (*yiaD*). Each entry was checked on the UniProtKB website for family and domain databases with default parameters (https://www.uniprot.org/). The *ompA* mutant was included as a negative control since its phenotype has been previously described[4,10,30–32]. Isogenic single-gene Tn26 insertion mutants in each locus and the parental wild-type (WT) strain AB5075_UW were acquired from the Manoil lab collection[33]; mutants were verified by PCR (Supplementary Table 1) and sequencing. Unfortunately, we achieved a negative PCR result for mutant ABUW_2571 (*dotU1*), which was excluded from the study. On Luria–Bertani (LB) agar plates, colony size, form, elevation, and margin did not differ between the WT and *ompA*-like mutants, except for the *ompA* mutant, which displayed a mucoid phenotype. A Protein BLAST pairwise alignment was performed between $OmpA_{AB5075}$ and each of the selected OmpA-like (https://blast.ncbi.nlm.nih.gov/); the retrieved scores of identity and similarity with YiaD were 45% (50/110) and 59% (65/110), ArfA 37% (41/110) and 58% (64/110), PsaB 33% (35/105) and 53% (56/105), respectively. Conversely, no similarity BLASTP scores could be retrieved comparing $OmpA_{AB5075}$ to CarO using default parameters. In addition, a multiple alignment showed that most identities/similarities were found within the C-terminal domain for all OmpA-like included, but CarO (Supplementary Fig. 1).

ompA-like mutations affect bacterial growth

To evaluate the effects of each *ompA*-like mutation on the bacterial growth, the WT, mutant, and complemented strains were cultured in LB broth up to the early stationary phase (Fig. 1A). All the *ompA*-like mutants displayed a growth defect, although to a different extent: on all measured time points for both *psaB* and *ompA* mutants, mainly in the exponential phase for *arfA* and *yiaD*, and during the mid-exponential phase in the case of *carO*. No significant difference was found among the WT, the WT carrying the empty vector (pA), and the complemented strains ($p > 0.05$). Since the growth temperature can influence phospholipid composition, which is in close contact with OMPs, we wanted to assess the impact of their lack on bacterial growth at a higher temperature. Therefore, WT, mutant, and complemented strains were cultured in LB at 42 °C, and bacterial viability was determined after 3 h (Fig. 1B). Compared to the WT, the rise in the temperature affected all *ompA*-like mutants but the *carO*-defective mutant. As expected, the *ompA* mutation deeply impacted bacterial growth, particularly at 42 °C[9,11–13], thereby confirming its essential role in *A. baumannii* physiology (Fig. 1). Therefore, PsaB and ArfA impair, to a lesser extent, the bacterial growth, while the lack of *yiaD* accelerates it at 42 °C. In contrast, the complemented strains exhibited no statistically significant difference compared to the WT and WT(pA) (Fig. 1B). To evaluate the mechanical properties of the OM in *ompA*-like mutants in comparison to the WT, bacterial growth was measured in bacteria-embedded in an LB-1% agarose matrix at 37 °C[34,35]. This matrix provides mechanical resistance to cell elongation, thereby determining cell stiffness; thus, the optical densities at 600 nm (OD_{600}) of cultures embedded in the LB agarose matrix could be linearly correlated with cell density[34,35]. OD_{600} values higher or lower than those of the WT indicate increased or decreased stiffness, respectively[34,35]. During the exponential phase, there were no significant differences among the strains; from then on, a statistically significant difference in growth rates was observed in the *carO* and *arfA* mutants, meaning a decreased and increased stiffness, respectively (Fig. 1C). Therefore, these data indicate that the absence of CarO and ArfA has opposite effects on the ability of the OM

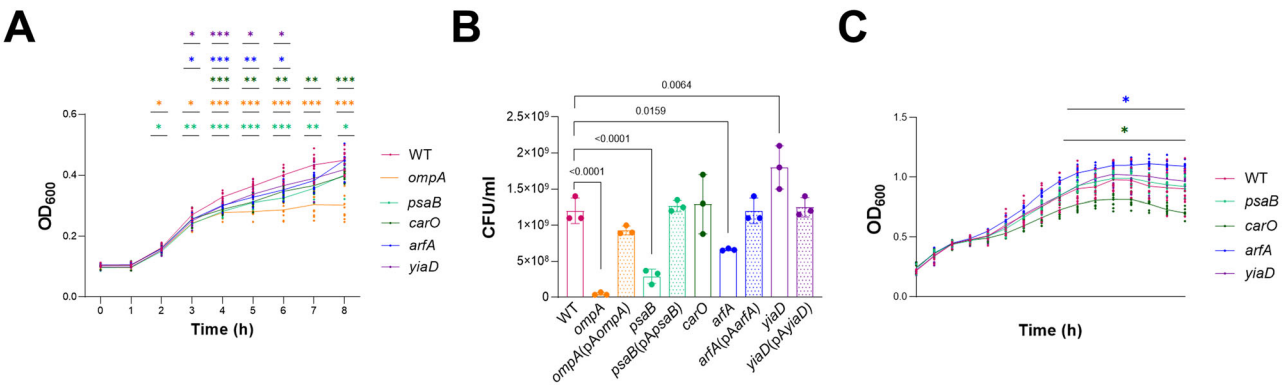

Fig. 1 | Growth kinetics of *ompA*-like mutants. The WT strain AB5075 (WT), mutant, and complemented strains were grown with shaking at the following conditions: **A** at 37 °C in LB broth for 8 h ($n = 10$); **B** at 42 °C in LB broth for 3 h ($n = 3$); and **C** at 37 °C on LB agarose 1% for 15 h ($n = 9$). OD_{600} values of each strain were recorded hourly, whereas CFU/ml was measured at the endpoint. Data are shown as means ± SDs. Statistical significance of one-way- and two-way ANOVA (color-code asterisks): $*p < 0.05$, $**p < 0.01$, and $***p < 0.001$.

Table 1 | Impact of the mutation in OmpA-like proteins on antibiotic susceptibility, assessed by broth microdilution assay

Class	Antibiotic	Strains*					
		WT	*ompA*	*psaB*	*carO*	*arfA*	*yiaD*
Penicillins	Ampicillin/sulbactam	>16/8	**8/4**	>16/8	>16/8	>16/8	>16/8
	Piperacillin	>64	**32**	>64	>64	>64	>64
	Piperacillin/tazocin	>64	64	>64	>64	>64	>64
	Ticarcillin	>64	>64	>64	>64	>64	>64
	Ticarcillin/clavulanate	>64	>64	>64	>64	>64	>64
Cephalosporins	Ceftazidime	>32	>32	>32	>32	>32	>32
	Cefotaxime	>64	>64	>64	>64	>64	>64
	Cefepime	>32	**8**	>32	>32	>32	>32
Aminoglycosides	Amikacin	>32	**8**	>32	>32	>32	>32
	Gentamicin	>8	**2**	>8	>8	>8	>8
	Tobramycin	>8	**≤2**	>8	8	>8	8
	Netilmicin	>8	**≤2**	>8	>8	>8	>8
Fluoroquinolones	Ciprofloxacin	>2	>2	>2	>2	>2	>2
	Levofloxacin	>4	**1**	4	4	>4	4
Carbapenems	Imipenem	8	4	8	8	8	8
	Meropenem	16	8	16	16	16	16
Tetracyclines	Tetracycline	≤2	**>8**	**>8**	**>8**	**>8**	**>8**
	Doxycycline	≤4	≤4	≤4	≤4	≤4	≤4
	Minocycline	≤2	≤2	≤2	≤2	≤2	≤2
Monobactams	Aztreonam	>16	>16	>16	>16	>16	>16
Polymyxins	Colistin	≤2	≤2	≤2	≤2	≤2	≤2
Sulfonamides	Sulfamethoxazole/trimethoprim	>4/76	>4/76	>4/76	>4/76	>4/76	>4/76
Fosfomycin	Fosfomycin	>64	≤32	64	64	>64	64

The minimum inhibitory concentration (MIC) for each antibiotic tested is given below each mutant.
*Significant changes in MIC values (differences ≥ 2 $\log_2$) are highlighted in bold.

to resist mechanical stress, thereby contributing to cell stiffness and integrity. The *ompA* mutant was excluded from this analysis since this assay is not recommended for strains with dissimilar growth curves[34,35]. Complementing strains *carO* and *arfA* with pA*carO* and pA*arfA*, respectively, restored the WT stiffness ($p > 0.05$) (data not shown).

ompA-like mutations do not change antibiotic susceptibility

The impact of each mutation on the minimum inhibitory concentration (MIC) was assessed by broth microdilution assay (Table 1). As expected, the *ompA* mutant showed MIC values significantly (differences ≥ 2 $\log_2$) lower, compared with the parental strain, for all aminoglycosides tested, penicillins (i.e., ampicillin/sulbactam, and piperacillin), cefepime, and levofloxacin. Conversely, no significant changes were observed for the other mutants. The increased MIC values for tetracycline in all mutants are due to the insertion of the Tn26 transposon[33]. These data indicate that each porin does not directly affect the OM antibiotic influx, apart from OmpA.

ompA-like mutations impact bacterial permeability and cell envelope thickness

It is known that a fluid OM forms a powerful barrier in gram-negative bacteria. A permeability assay was performed to test the effect of the lack of OmpA-like proteins on OM. DAPI (4′,6-diamidino-2-phenylindole (DAPI)) is an impermeable, blue fluorescent DNA stain mostly excluded from the intact membrane. However, it can enter compromised membranes and bind intracellular DNA. Hence, we measured the DAPI cell permeability of *ompA*-like mutants compared to the WT (Fig. 2A, B). Killed bacteria (KB) were used as positive controls. Despite the potential of DAPI to be a substrate for efflux pumps, statistically significant differences were observed between the WT and the *ompA*, *psaB*, and *yiaD* mutants (Fig. 2B). The permeability defect was restored in the complemented mutants (Fig. 2B). Thus, the absence of these proteins has a dominant-negative effect on OM permeability, possibly due to a defect in the fluidity of the OM. To assess whether this defect could impact on the entire cell envelope, including the OM, peptidoglycan, and inner membrane, we performed transmission electron microscopy (TEM) measurements to determine the thickness of the cell envelope in *ompA*-like mutants. Noteworthy, 6% of the *arfA* mutant cells showed the most aberrant morphology with a morphotype of a typical cell division defect (Fig. 2C). In contrast, the other *ompA*-like mutants retained a shape comparable to WT (Fig. 2C). Interestingly, measurements of cell envelope thickness demonstrated a thickness reduction in *arfA* > *yiaD* > *psaB* mutants (Fig. 2D); a change in cell envelope thickness could affect the physical properties of the bacterial cells. Complementation of each mutant with the missing gene restored the WT cell envelope thickness and morphology (Fig. 2 and Supplementary Fig. 2). Overall, these results link the reduced thickness of the cell to increased permeability to DAPI in both *psaB* and *yiaD* mutants while maintaining an antibiotic susceptibility profile comparable to the WT (Table 1).

ompA-like mutations have dramatic effects on adhesion, virulence, and motility

Cell-surface hydrophobicity is tightly associated with motility, biofilm formation, and cell adhesion[36]. The salt aggregation test was performed to evaluate cell-surface hydrophobicity[37]. The underlying principle is based on the evidence that increasing salt concentrations cause bacterial aggregation due to hydrophobic and cell–protein interactions, thus indirectly measuring the surface hydrophobicity; the most hydrophobic cells are the first to precipitate at a low salt concentration[37]. The assay with different concentrations of ammonium sulfate was performed on glass slides, and optical microscopy images were acquired (Fig. 3A). It has been reported that International Clone I (IC I) strains, such as AB5075, aggregate in the range

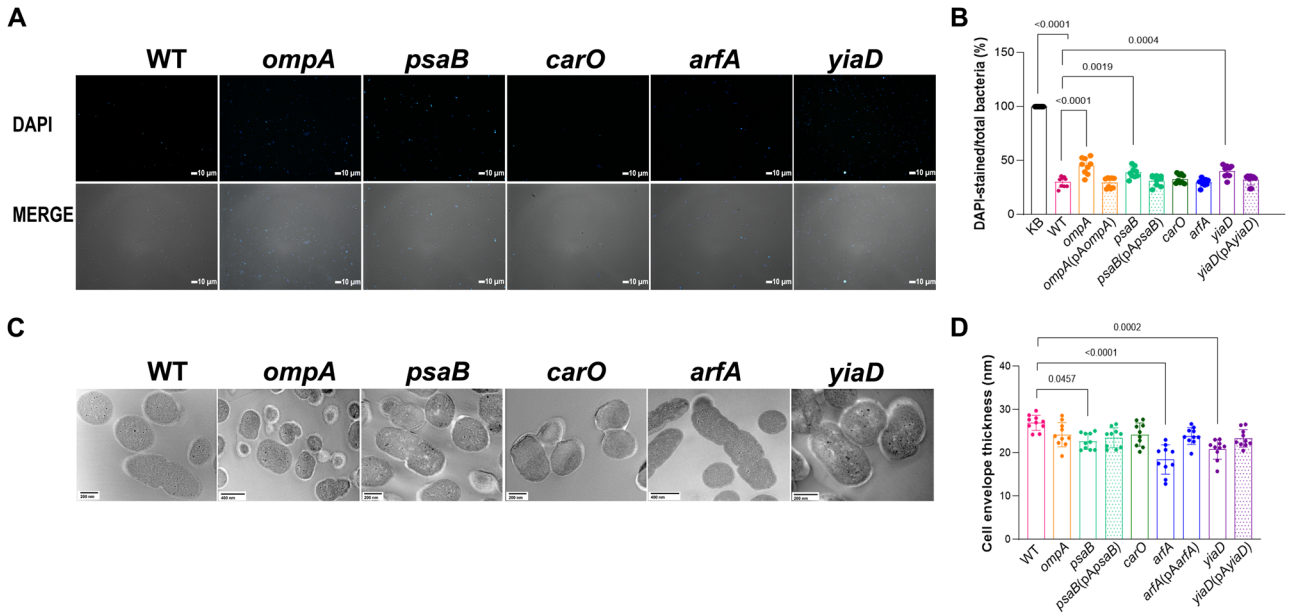

Fig. 2 | Cell permeability and cell envelope thickness of *ompA*-like mutants. **A** Bacteria were incubated with DAPI, washed, centrifuged on polylysine-treated coverslips, and mounted for fluorescence microscopic analyses. Bright-field pictures were merged with fluorescence images. **B** Quantification of DAPI stained bacteria, with KB used as the positive control ($n = 9$). **C** TEM images of bacteria cells grown to exponential phase. **D** The average cell wall thickness of each strain was assessed by TEM ($n = 60$). Representative images of four experiments at different magnifications are shown. Data are shown as means ± SDs. Statistical significance was evaluated by one-way ANOVA.

of salt between 0.5 M and 1 M[38]. Indeed, the aggregation of the WT agrees with previous results on IC I. Differently from the WT and the *psaB* mutant that aggregated rapidly even at low $(NH_4)_2SO_4$ concentrations, *carO* and *yiaD* mutants displayed aggregation only at higher concentrations with the *arfA* only to the highest (Fig. 3A). Conversely, the *ompA* mutant exhibited no aggregation (Fig. 3A). No differences from the WT and WT(pA) could be detected in the aggregation patterns of the complemented mutants (Supplementary Fig. 3). These results indicated that the lack of PsaB does not impact on bacterial cell-surface hydrophobicity. In contrast, the other proteins retained this feature to a lesser extent in the following order: CarO and YiaD > ArfA > OmpA.

Despite its name, *A. baumannii* exhibits surface-associated motility associated with OMPs, among other encoded genes[1,39,40]. Thus, the involvement of the OmpA-like proteins in surface-associated motility was evaluated. Differently from the WT, motility was abrogated in all mutants (Fig. 3B). Introduction of the missing genes with plasmid pA partially restored the WT motility phenotype (Fig. 3B). Thereafter, the ability of *ompA*-like mutants to form biofilm was assessed. A statistically significant decrease of the biofilm-forming ability was observed only for the *ompA* and *arfA* mutants (Fig. 3C), in agreement with the decreased cell surface hydrophobicity (Fig. 3A). In addition, the adhesiveness to human A549 epithelial lung cells was investigated. Results showed a significant decrease in the adhesion to host cells by all mutants but the *psaB* mutant (Fig. 3D). Finally, WT and mutant strains were comparatively assessed for in vivo virulence using the *Galleria mellonella* systemic infection model. The LD_{50} for *A. baumannii* WT AB505 strains was 10^5 colony-forming unit (CFU)/larva (Supplementary Fig. 4A). Results showed that the WT strain is the most virulent among those tested (Fig. 3E and Supplementary Table 2). In addition, *carO* and *arfA* mutants resulted in being significantly more virulent compared with *psaB* ($p < 0.05$) and *yiaD* ($p < 0.001$) mutant strains. A general time-dependent virulence trend was observed for all strains except for *ompA*, which was completely avirulent, showing a survival curve comparable to those of control larvae [unexposed, and phosphate-buffered saline solution (PBS)-administered] as previously described[41]. Therefore, the hierarchy of virulence observed among the mutants tested from least to most virulent was *ompA* > *yiaD* > *psaB* > *carO* > *arfA*. The in vivo virulence was restored to almost WT levels in the complemented strains; although not fully restored in the complemented *yiaD* mutant, in vivo virulence was significantly increased (Supplementary Fig. 4B). Overall, data demonstrated that PsaB, CarO, ArfA, and YiaD are involved in surface-associated motility, a phenotype that does not seem associated with cell-surface hydrophobicity. In agreement with previous data[42], CarO promotes cell adhesion and is involved in in vivo virulence, thereby demonstrating a prominent role in host interaction, as previously observed[25,42]. Interestingly, ArfA plays a role in all virulence traits analyzed; the decrease of cell surface hydrophobicity slightly affected the biofilm-forming activity and the in vivo virulence, while its absence increased the bacterial adhesiveness to host cells. Furthermore, in our experimental conditions, YiaD was not involved in biofilm formation[29]; however, data showed that YiaD plays a role in both in vitro and in vivo virulence, a previously not investigated feature.

The OmpA-like protein PsaB negatively correlated to stress tolerance

A. baumannii shows an intrinsic aptitude to persist in nosocomial and community settings, indicating its great capability to tolerate environmental stresses. To analyze the contribution of OmpA-like proteins to external stress tolerance, the growth of *ompA*-like mutants was evaluated under different stress conditions (Fig. 4). The *psaB* mutant showed an increased survival rate to all stress conditions, but meropenem. Resistance to the membrane disrupter antibiotic zeocin was also assayed; in accordance with the antibiogram profiles, resistance to zeocin did not affect *ompA*-like mutants (Fig. 4F). In line with previous observations[29], the *yiaD* mutant showed increased resistance to meropenem; complementing this mutant with the *yiaD* gene increased its susceptibility to meropenem to WT levels, thereby confirming its role in meropenem sensitivity of *A. baumannii* (Fig. 4G)[29]. Apart from the *ompA* and *carO* mutants, all the other *ompA*-like mutants showed increased resistance to human serum (Fig. 4H). In comparison to WT, the most serum-resistant mutants were *yiaD* > *arfA* > *psaB*; the rates of resistance after 2 h of incubation were 4,473-, 318- and 245-fold higher than the WT, respectively, and 618-, 11-, and 42-fold more elevated than the WT, respectively, after 4 h (Fig. 4H). Therefore, it seems that the

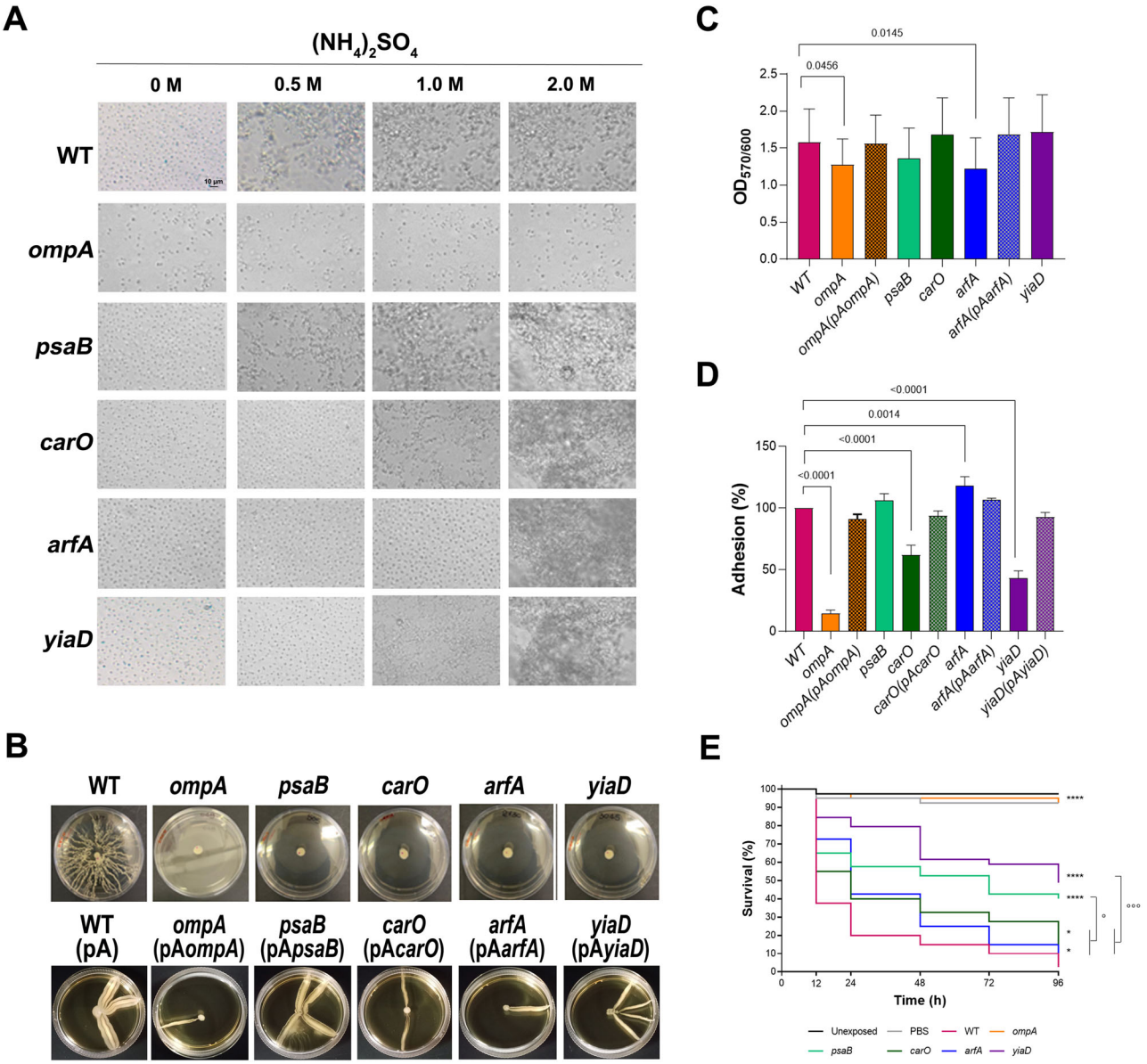

Fig. 3 | Cell-surface hydrophobicity, motility, biofilm formation, adhesion to host cells, and in vivo virulence of *ompA*-like mutants. A Representative microscopic images (40×) of bacterial cell aggregation of mutants and WT after exposure to increasing concentrations of ammonium sulfate. **B** Representative images of surface-associated motility of each mutant and WT assayed on semisolid (0.25%) LB agar plates. **C** Amount of biofilm formed by each mutant and WT ($n = 30$), as measured by crystal violet stain in a 96-well tissue culture plate. **D** Adhesion of each mutant and WT to human A549 lung epithelial cell monolayers infected using a MOI of 10. Cell-surface-adherent bacteria were enumerated after 2.5-h incubation ($n = 3$). Data are shown as means ± SDs. Statistical significance was evaluated by one-way ANOVA. **E** In vivo, virulence was assessed in *G. mellonella* larvae peritoneally injected with 10^5 CFU and scored for mortality over 96 h ($n = 40$). In this panel, statistical significance was evaluated with a Log-rank Mantel–Cox test: $^{*}p < 0.05$, $^{**}p < 0.01$, $^{***}p < 0.001$, and $^{****}p < 0.0001$, vs WT strain; $^{\circ}p < 0.05$, and $^{\circ\circ\circ}p < 0.001$.

lack of *yiaD* confers a substantial advantage during growth in human serum. Susceptibility to ethanol, low pH, high salinity, Triton X-100, and chlorpromazine was restored in the *psaB* mutant complemented with pA*psaB* (Fig. 4). Complemented mutants reverted to WT tolerance levels upon exposure to fresh human sera (Fig. 4H).

Discussion

The fast-rising rates of extensively and pan-drug resistant *A. baumannii* strains require urgently new therapeutic options. Due to its critical role in *A. baumannii* pathogenicity, OmpA is still considered the primary target for designing innovative therapies[4–8]. This study focuses on lesser and unknown OmpA-like proteins in *A. baumannii* AB5075, aiming to identify potential novel drug and vaccine targets.

The results presented in this study are summarized in Fig. 5. Loss of *ompA*-like porins showed pleiotropic effects, mainly impacting bacterial growth, surface-associated motility, and in vivo virulence, although to different extents among mutants (Figs. 1, 2, and 5). Conversely, the antibiotic susceptibility was almost unaffected by the absence of these porins except for the *ompA* mutant, which displayed an altered phenotype in line with previous observations[13,25].

The permeability defect showed in both *psaB* and *yiaD* mutants indicates that these porins are directly involved in preserving the typical selective permeability of the OM in gram-negative bacteria (Figs. 2 and 5). A stable lipopolysaccharide (LPS) layer represents the second dominant structure affecting OM permeability, following OMPs[43]. The abundant LPS molecules carry a net negative charge partly neutralized by divalent cations

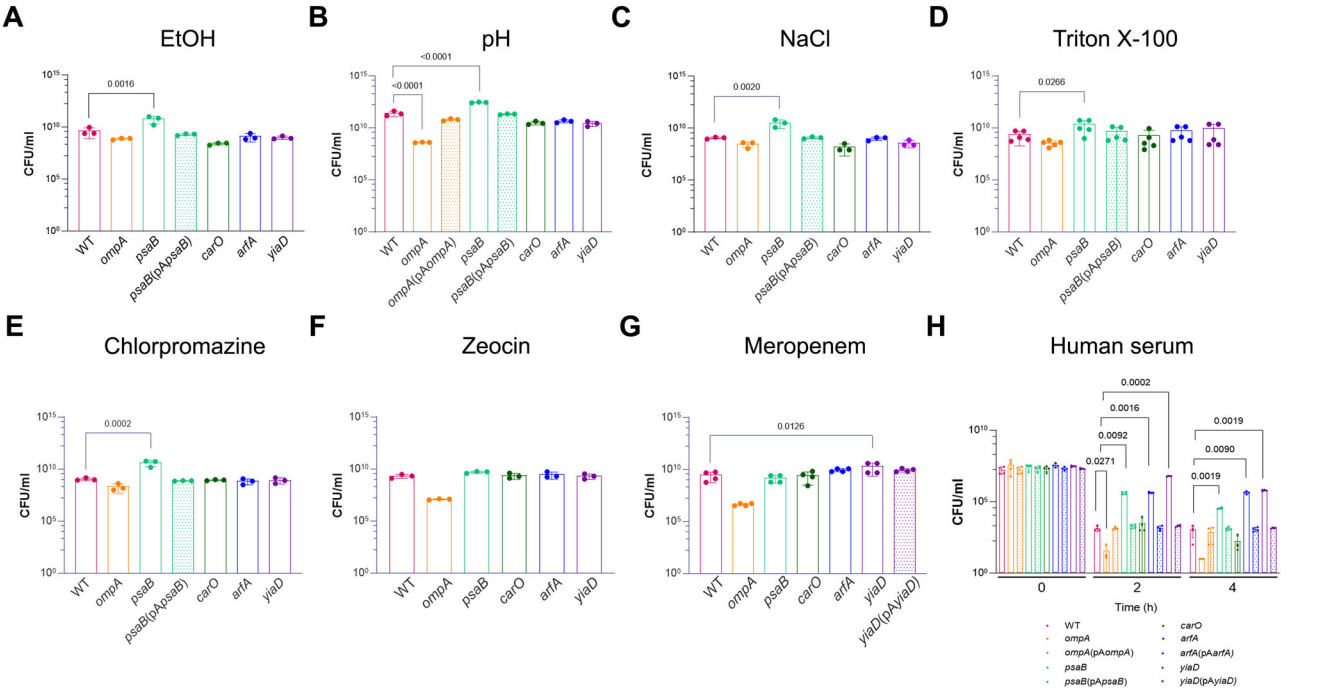

Fig. 4 | Stress tolerance of *ompA*-like mutants. The effect of *ompA*-like mutations on tolerance to growth stresses was evaluated on agar plates supplemented with **A** ethanol 4% ($n = 3$), **B** pH 6.0 ($n = 3$), **C** NaCl 20 g/l ($n = 3$), **D** Triton X-100 1% ($n = 5$), **E** chlorpromazine 16 µg/ml ($n = 3$), **F** zeocin 25 µg/ml ($n = 3$), **G** meropenem 4 µg/ml ($n = 4$). **H** Tolerance to human serum was evaluated by exposing bacteria (5×105 CFU/ml) to 100% human serum and incubating at 37 °C for 2 h and 4 h before CFU/ml counting ($n = 4$). Data ($\log_{10}$) are shown as means ± SDs. Statistical significance was evaluated by one- and two-way ANOVA.

Fig. 5 | Heat map representing the functional characterization of *A. baumannii* OmpA-like proteins. The role of each gene in bacterial physiology, virulence, and stress tolerance was assessed by different methods, as previously described. The color code represents the relationship with WT data, based on *p* values, with blue and pink highlighting that mutants were more defective or proficient, respectively, compared to the WT for each specific feature. The darkness of the color is directly proportional to the statistical significance value. White boxes indicate no statistical difference compared to the WT strain.

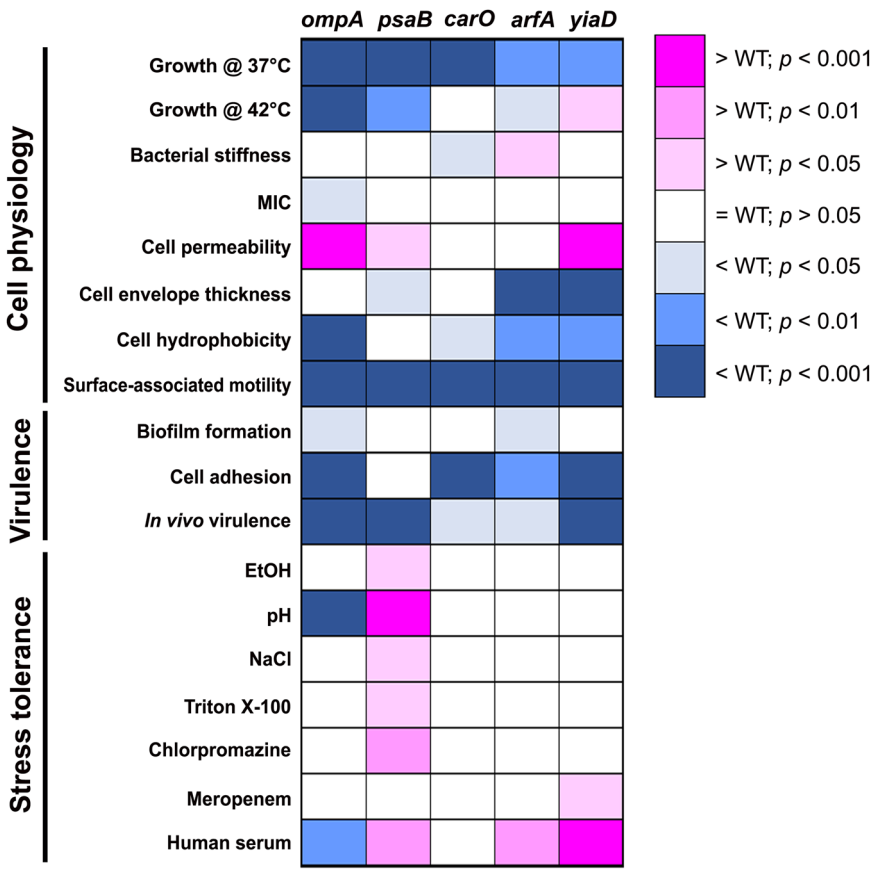

(i.e., Ca^{2+}, Mg^{2+})[43,44]. Alteration in OMPs, disordered LPS networks, and charge changes can increase permeability[43,44]. These proteins showed a high degree of identity with OmpA in the C-terminal domain, suggesting a role in supporting OmpA in cell mechanics. In *Escherichia coli*, many OMPs bind the cell wall with their OmpA-like C-terminal domain[45–47]. This connection significantly impacts on the architecture and physiological features of the whole cell envelope. These aspects are crucial for maintaining mechanical integrity, viability, cellular fitness, motility, stress survival, and virulence. In addition, the interaction between OMPs and the cell envelope defines the bacterial shape, sustains mechanical loads such as turgor pressure, and withstands physical stresses[43,44,46]. Therefore, through OMP content and amount, the permeability of the OM barrier adapts to the extracellular environmental stimuli to improve fitness and survival, a phenomenon known as stiffness tunability[43,44,46].

The 18 kDa PsaB protein is highly conserved among *Acinetobacter* spp. According to STRING, it is supposed to interact with the TolB–Pal of the Tol–Pal system proteins. In *E. coli*, TolB physically interacts with lipoproteins Pal and Lpp as well as OmpA, and Pal with OmpA[48]. Previous studies demonstrated that mutations in *tol/pal* genes in *E. coli* and *Salmonella* affect OM integrity and motility[49–51]. Therefore, we speculate that the absence of *psaB* impacts on the TolB–Pal proteins, affecting OM integrity and abrogating surface-associated motility. The observed increased OM permeability and decreased cell envelope thickness support our hypothesis. On the other hand, the extraordinary tolerance of the *psaB* mutant to all the stresses tested indicates that PsaB is responsible for *A. baumannii* membrane fluidity in response to stressors. Physiologically, decreasing expression of *psaB* leads to enhanced tolerance to different stresses, including ethanol, low pH, detergent, ionic strength, efflux pump inhibitors, and human serum (Figs. 4 and 5). In *E. coli*, the expression levels of OmpF and LamB decrease to enhance organic solvent tolerance[52]. *Pseudomonas stutzeri* mutants resistant to polycationic compounds showed a heavy alteration in OMPs profile, although modifications appeared to be strain-specific[53]. Hence, the levels of *psaB* expression under stressful growth conditions in the WT warrant future studies. Moreover, the *psaB*, *yiaD*, and *arfA* mutants showed a decreased cell envelope thickness, even though these mutants exhibit a variable hydrophobicity (Figs. 2, 3, and 5). In particular, the *arfA* mutant displayed an aberrant cell shape in approximately 6% of the total bacterial population and a significantly increased stiffness compared to the other mutants in the agarose test (Figs. 1, 2, and 5). The lack of interactions between its C-terminal domain and the cell wall due to the loss of ArfA might reduce the space between OM and the peptidoglycan. Consequently, this effect increases bacterial stiffness and reduces the water content, shrinking the thickness of the cell envelope, as previously reported for *E. coli*[54]. Overall, we suggest that in *A. baumannii*, ArfA has a main role in the interaction with the cell wall, OM fluidity, cell shape, cell surface hydrophobicity, and to a lesser extent in biofilm formation, and in vivo virulence.

CarO, the second most studied porin in *A. baumannii*[25], was initially identified as responsible for the entry of imipenem[22]. The prevalence of *carO*-defective clinical isolates underscored its apparent dispensability in *A. baumannii* physiology[25]. Our findings align with previous reports, demonstrating that CarO contributes to bacterial surface hydrophobicity, host cell adhesion, and in vivo virulence[42,55]. Indeed, among the different *ompA*-like mutants analyzed, the *carO* defective strain showed the more nuanced phenotype, empathizing with the remarkable adaptive strategies reported for the *carO* mutants.

Another excellent example of *A. baumannii's* adaptability comes from YiaD. It has been recently reported that expression of YiaD is downregulated after exposure to meropenem, a commonly used carbapenem in the clinic[29]. Accordingly, an increase in the resistance to meropenem was observed in the *yiaD* mutant (Figs. 4 and 5), thus confirming the ability of *A. baumannii* to cope with stresses by varying the content of OMPs to fit a harsh environment better and survive.

Interestingly, like the *ompA* mutant[56,57], the *ompA*-like mutants lost surface-associated motility, a typical feature of *A. baumannii* belonging to the IC I[38]. This indicates that they all play a role in stabilizing the OM structure to sustain surface-associated motility (Figs. 3 and 5).

Cell surface hydrophobicity is essential for bacterial lifestyles, mitigating initial repulsive forces between bacteria and surfaces[36]. This trait is pivotal for host cell adhesion, biofilm formation, and motility. Previous studies on clinical *A. baumannii* strains showed that strains with higher hydrophobicity were associated with increased biofilm production and motility but reduced virulence compared to less hydrophobic strains[38,58]. Our results on the *arfA, yiaD*, and *carO* mutants are in accordance with this phenotypic association, although to different extents (Figs. 3 and 5). Besides their structural role within the OM, these OMPs likely contribute to maintaining the surface hydrophobicity needed for the initial bacterial contact with abiotic substrates, thus influencing surface-associated motility, biofilm formation, as well as virulence.

A. baumannii clinical isolates often lead to severe bacteremia, displaying remarkable resistance to human sera[59]. Besides OmpA, other complement resistance genes were identified as essential for *A. baumannii* human serum survival, including the *mla* pathway encoding proteins responsible for OM asymmetry[14,59,60]. Herein, we showed an increased serum resistance in the *psaB*, *yiaD*, and *arfA* mutants (Fig. 4H). Interestingly, it was reported that *mla* mutants were characterized by an increased OM permeability[14,60]; accordingly, also the loss of PsaB and YiaD caused an increased permeability to DAPI, differently from the *arfA* mutant (Fig. 2). In addition to the increased serum-resistance, *A. baumannii ompA*-like mutants showed a significantly decreased ability in cell adhesion and virulence (Figs. 3 and 5). Bacterial OMPs play a crucial role in host interactions and are generally referred to as virulence-related OMPs. For instance, OmpX in *E. coli*, Rck in *Salmonella enterica* serovar Typhimurium, and Ail in *Yersinia enterocolitica* were shown to promote cell adhesion and invasion and defend against the complement system[61,62]. The contradictory findings regarding the reduced in vivo virulence and increased serum resistance observed in the *yiaD* mutant, in comparison with the WT, recall those observed for the OmpC protein from *E. coli*[63–65]. These studies revealed the dual role of OmpC as a target for the complement classical pathway and as an adhesin[63–65]. Consequently, the absence of OmpC justifiably contributes to the reported phenotypic characteristics[63–65]. These findings strongly suggest that YiaD may also play analogous roles. Considering the *arfA* mutant phenotype patterns, ArfA appears to play a crucial role in maintaining cell envelope integrity, including cell shape, OM fluidity, and surface hydrophobicity. Hence, it can be inferred that these OMPs could serve as targets for the complement system, and the bacterium may fine-tune their expression during bacteremia to evade the bactericidal effects of the complement cascade. Based on our results, we propose classifying PsaB and YiaD, similarly to OmpA, as virulence-related OMPs in *A. baumannii*. While ArfA plays a significant role in shaping cell architecture and physiology, its contribution to virulence appears comparatively less pronounced than that of PsaB and YiaD. Future studies will address in more detail the binding target(s) of the protruding loops of these OMPs.

Conclusions

In gram-negative bacteria, maintaining OM homeostasis and critical cellular functions relies on OMPs and lipoproteins and their interaction with the cell wall. These fundamental structural mechanical properties control cell shape, growth and division, and stress protection[25,43–45]. OMP redundancy guarantees and preserves OM integrity and allows them to fine-tune their expression depending on external stimuli. These proteins, representing major virulent factors and being surface exposed, are prime targets for controlling *A. baumannii* pathogenesis and environmental persistence. Despite considerable progress in understanding *A. baumannii* physiology and virulence, several OMPs still need to be more detailed. Identifying and characterizing proteins essential for cell physiology, survival, persistence, and virulence may have a massive impact on designing novel targets and strategies for innovative therapeutics against extensively and pan-drug resistant *A. baumannii*.

This study focused on characterizing OmpA-like proteins in *A. baumannii* AB5075. Apart from YiaD, no role in the transport of antibiotics was detected among OmpA-like proteins. Conversely, a significant impact on bacterial physiology (i.e., OM integrity, motility, and cell surface hydrophobicity) and virulence (i.e., biofilm-forming activity, host cell adhesion, in vivo virulence, and serum tolerance) was shown for each OMP, although to a different extent. Notably, PsaB was found to correlate negatively with stress tolerance. We propose classifying PsaB and YiaD, similarly to OmpA, as virulence-related OMPs in *A. baumannii*. Instead, ArfA primarily maintains the bacterial cell's structural integrity and physicochemical properties. Overall, this study provides important insights into the specific roles of these porins in the physiology and virulence of *A. baumannii*. Further research will elucidate the expression profile patterns of these OMPs during stress exposure and host-cell interaction.

Methods

Bacterial strains, generation of complemented strains, and growth conditions

The *A. baumannii* AB5075-UW reference, WT strain, and Tn26 *ompA*-like mutants were provided by BEI Resources (Manassas, VA, USA). Mutants were checked by PCR using T26 internal and specific primers (listed in Supplementary Table 1) and a Tm of 58 °C. For in-trans complementation, the aminoglycoside 3-*N*-acetyltransferase type 4 (*aac4*) gene was inserted EcoRV/BamHI into the *E. coli-Acinetobacter* species shuttle-vector pWH1266[66], generating plasmid pA. Each *ompA*-like gene was PCR amplified using specific primers (Supplementary Table 1) and cloned into the PstI or ScaI/EcoRI restriction sites of the pA plasmid, generating pA*psaB*, pA*ompA*, pA*carO*, pA*arfA* and pA*yiaD*. Subsequently, the complementing plasmids were electroporated into their respective mutant strains and selected on LA supplemented with 50 µg/ml apramycin (Sigma Aldrich, Italy). All amplicons were sequenced (Bio-Fab Research, Rome, Italy). To confirm plasmid transformation, specific PCR and plasmid restriction analyses were performed. Routine growth and plating were carried out in LB broth and 1.5% agar plates (Oxoid, Milan, Italy). Opaque colonies were distinguished under oblique lighting and used during the mid-exponential growth phase at a cell density (OD_{600}) equal to 0.8.

Growth kinetics

The growth kinetics of the WT, the mutants, and the complemented strains were determined in LB broth at 37 °C and 42 °C in microtiters and in flasks under dynamic conditions (200 rpm), respectively. OD_{600} was determined every hour over an 8-h period using a 7315 spectrophotometer Jenway. Two independent experiments, five wells per strain, were performed ($n = 10$). Bacterial serial dilutions were spotted on LA after 3 h and CFU/ml were enumerated after 12 h of incubation at 37 °C. For these experiments, three independent experiments were performed ($n = 3$).

MIC assay

Antimicrobial susceptibility testing was performed with 100 µl of a 0.5 McFarland bacterial suspension using the WalkAway plus System (Beckman Coulter, Pasadena, CA) and interpreted according to the European Committee on Antimicrobial Susceptibility Testing (EUCAST 2022), as reported elsewhere[67].

Surface-associated motility assay

The surface-associated motility was investigated as previously described[68,69]. Briefly, a single opaque colony of the WT, the mutants, and the complemented strains were cultured overnight at 37 °C under dynamic conditions (200 rpm). Thereafter, 5 µl of each bacterial culture at stationary phase ($OD_{600} > 2$) were spotted in the center of low-percentage (0.25%) agar (Oxoid, ThermoFisher, Italy) plates. Plates were incubated at 37 °C for 16 h and photographed. Three independent experiments, two plates per strain, were performed ($n = 6$).

Salt aggregation test

The surface hydrophobicity of mutants and complemented strains was assessed by salt aggregation test, using the WT strain as control[70]. Briefly, single colonies were resuspended in 500 µl of double distilled water, and 25 µl were mixed with an equal volume of $(NH_4)_2SO_4$ solution of varying molarities (from 0 M to 2 M). After incubation, bacteria were spotted onto polylysine–coated coverslips (Sigma Aldrich), centrifuged, and photographed under a light microscope (Motik AE21 microscopy, Italy) at 40 × magnification. The bacterial cell surface was classified as: ≥0.5 M, highly aggregative or strongly hydrophobic, 1.0 M, 1.0–2.0 M, low aggregative or moderately hydrophobic, >2.0 M, non-aggregative or hydrophilic. Three independent experiments, in duplicate, were performed ($n = 6$).

Biofilm assay

Biofilm formation was measured using the microtiter plate assay, as previously described[69,71]. Briefly, overnight cultures were diluted 1:100 in LB and dispensed into 96-well polystyrene microtiter plates (Costar, Corning Inc., Sigma Aldrich) and incubated at 37 °C for 24 h under static conditions. Following OD_{600} measurements, plates were washed three times with PBS, fixed with methanol for 20 min at room temperature, and stained with 0.1% crystal violet solution for 15 min. After four additional washes, the surface-associated dye was solubilized with 200 µl of 95% ethanol and OD_{570} was recorded. Results are reported as the OD_{570}/OD_{600} ratio. Three independent experiments, ten wells per strain, were performed ($n = 30$). Isolates were classified as biofilm-forming if they yielded ratio values that were at least three standard deviations above that of the uninoculated medium, considered as the negative control[69,71].

Permeability assay

Exponentially grown bacteria were normalized by OD_{600}, washed twice with PBS, and DAPI was added at a final 2 µg/ml concentration. After 20 min of head-over-head rotation, samples were washed with PBS, and absorbance was detected using a CLARIOstar fluorescence microplate reader (BMG Labtech, Germany). From the same samples, 10 µl were spotted on coverslips, and images were acquired with a Leica DM5000B microscope equipped with the digital FireWire color camera system Leica DFX300 (Leica, Milan, Italy). Three independent experiments, in triplicate, were performed ($n = 9$).

Stress tolerance assays

Exponentially grown bacteria were normalized at OD_{600} of 0.8 and spotted on LB agar plates containing 4% ethanol (Carlo Erba srl, Milan, Italy), 16 µg/ml chlorpromazine, 4 µg/ml meropenem, 1% Triton X-100, 342 mM NaCl (all from Sigma Aldrich). To evaluate the temperature effects, bacteria were incubated at 25 and 42 °C, while the effects of pH were evaluated by spotting the bacteria on LB agar at pH 6.0 and 8.0. Finally, to assess the impact of the human serum, normalized bacteria were pelleted washed twice with PBS, and 5×10^5 CFU/ml were incubated in 100% human serum (EuroClone SpA, Milan, Italy) at 37 °C for 2 and 4 h[59]. Tolerance was assessed by determining the number of CFU/ml before and after serum incubation. Three to five independent experiments were performed ($n = 3$–5 as shown).

Bacterial stiffness

Bacterial stiffness was measured by comparing the growth of WT and mutants in LB or embedded in 1% agarose in 96-well plates. Growth data were collected over 15 h at 37 °C[35]. Three independent experiments, in triplicate, were performed ($n = 9$).

Adhesion assay

The human A549 lung epithelial cell type II line (ATCC CCL185; LGC Standards, Sesto San Giovanni, Italy) was used for adhesion assays. Cells were cultured in Dulbecco's modified Eagle's medium (DMEM) supplemented with 10% (*v*/*v*) heat-inactivated fetal bovine serum (FBS; Gibco, Milan, Italy), and 2mM L-glutamine, at 37 °C in a humidified atmosphere with 5% CO_2. Confluent monolayers were infected at a multiplicity of

infection (MOI) of 10, centrifuged at 700×*g* for 10 min, incubated for 2.5 h at 37 °C in 5% CO_2, and washed 10 times with PBS. Cell monolayers were lysed with 0.1% Triton X-100 to recover adherent bacteria, and serially diluted lysates were plated on LB agar plates to determine the number of adherent bacteria (CFU/ml). Due to the low invasive rates of strain AB5075[72], we considered the number of intracellular bacteria after 2.5 h of infection negligible. Three independent experiments were performed ($n = 3$).

In vivo virulence assay

The in vivo virulence was assessed in the wax moth larvae of *G. mellonella*. Exponentially grown strains were evaluated by infecting each larva with LD_{50}, and the number of dead caterpillars was scored at different times (18 h, 24 h, 48 h, 72 h, and 96 h), as previously described[73]. Control groups consisted of (i) larvae injected with PBS only and (ii) uninjected larvae. Each group consisted of 20 larvae purchased from Euro Esche (Quinzano d'Oglio, Brescia, Italy).

Evaluation of cell envelope thickness assay

Overnight cultures were pelleted, washed twice in PBS, and fixed in 2.5% glutaraldehyde/PBS for 48 h at 4 °C. Samples were pelleted and washed in 0.2 M sodium cacodylate buffer, resuspended in 2% osmium tetroxide for 2 h at room temperature, and embedded in EPON resin following a standard schedule. After overnight incubation at 65 °C, specimens were sectioned to 80 nm, using a Leica UC7 ultramicrotome (Leica Microsystems, Wetzlar, Germany), and mounted onto 200 mesh copper grids for TEM imaging (JEOL 1400 plus, Italy)[74]. Morphometric evaluation of the cell envelope thickness was calculated by measuring the space from the inner to the OM of 10 bacteria in 6 fields from TEM micrographs at the same magnification ($n = 60$), as previously reported[75].

Statistics and reproducibility

Normal distribution was determined with the Shapiro-Wilk test. The statistical differences of normally distributed data were analyzed with one- or two-way analysis of variance (ANOVA) for multiple comparisons and Student's *t*-test to compare two groups. The Log-rank Mantel–Cox test assessed differences in *G. mellonella* survival trends between groups. p values < 0.05 were taken as being statistically significant. Experiments were performed in independent replicates, as indicated, and similar results were obtained for all.

Reporting summary

Further information on research design is available in the Nature Portfolio Reporting Summary linked to this article.

Data availability

Data can be retrieved from *A. baumannii* AB5075 complete genome https://www.ncbi.nlm.nih.gov/nucleotide/CP008706, https://www.uniprot.org/, and https://blast.ncbi.nlm.nih.gov/. Additional data of this study are available within the supplementary data 1. All the other data are available from the corresponding author on reasonable request.

Received: 12 July 2023; Accepted: 29 July 2024;
Published online: 06 August 2024

References

1. Sarshar, M., Behzadi, P., Scribano, D., Palamara, A. T. & Ambrosi, C. *Acinetobacter baumannii*: an ancient commensal with weapons of a pathogen. *Pathogens* **10**, 387 (2021).
2. Vivo, A. et al. Epidemiology and outcomes associated with carbapenem-resistant *Acinetobacter baumannii* and carbapenem-resistant *Pseudomonas aeruginosa*: a retrospective cohort study. *BMC Infect. Dis.* **22**, 491 (2022).
3. Stracquadanio, S. et al. *Acinetobacter baumannii* and Cefiderocol, between cidality and adaptability. *Microbiol. Spectr.* **10**, e02347–02322 (2022).
4. Nie, D. et al. Outer membrane protein A (OmpA) as a potential therapeutic target for *Acinetobacter baumannii* infection. *J. Biomed. Sci.* **27**, 1–8 (2020).
5. Ansari, H., Tahmasebi-Birgani, M., Bijanzadeh, M., Doosti, A. & Kargar, M. Study of the immunogenicity of outer membrane protein A (ompA) gene from *Acinetobacter baumannii* as DNA vaccine candidate in vivo. *Iran. J. basic Med. Sci.* **22**, 669 (2019).
6. Tamehri, M. et al. Combination of BauA and OmpA elicit immunoprotection against *Acinetobacter baumannii* in a murine sepsis model. *Microb. Pathog.* **173**, 105874 (2022).
7. Sogasu, D., Girija, A. S., Gunasekaran, S. & Priyadharsini, J. V. Molecular characterization and epitope-based vaccine predictions for ompA gene associated with biofilm formation in multidrug-resistant strains of *A. baumannii*. *Silico Pharmacol.* **9**, 1–11 (2021).
8. Ghanipour, F., Nazari, R., Aghaee, S. S. & Jafari, P. Evaluation of the antimicrobial ability of probiotics against nosocomial infections by inhibiting Ompa gene expression in *Acinetobacter Baumannii*. *J. Arak Univ. Med. Sci.* **24**, 854–867 (2022).
9. Iyer, R., Moussa, S. H., Durand-Reville, T. F., Tommasi, R. & Miller, A. *Acinetobacter baumannii* OmpA is a selective antibiotic permeant porin. *ACS Infect. Dis.* **4**, 373–381 (2017).
10. Gaddy, J. A., Tomaras, A. P. & Actis, L. A. The *Acinetobacter baumannii* 19606 OmpA protein plays a role in biofilm formation on abiotic surfaces and in the interaction of this pathogen with eukaryotic cells. *Infect. Immun.* **77**, 3150–3160 (2009).
11. Kwon, H. I. et al. Outer membrane protein A contributes to antimicrobial resistance of *Acinetobacter baumannii* through the OmpA-like domain. *J. Antimicrobial Chemother.* **72**, 3012–3015 (2017).
12. Park, J. S. et al. Mechanism of anchoring of OmpA protein to the cell wall peptidoglycan of the gram-negative bacterial outer membrane. *FASEB J.* **26**, 219 (2012).
13. Skerniškytė, J. et al. The mutation of conservative Asp268 residue in the peptidoglycan-associated domain of the OmpA protein affects multiple *Acinetobacter baumannii* virulence characteristics. *Molecules* **24**, 1972 (2019).
14. Kim, S. W. et al. Serum resistance of *Acinetobacter baumannii* through the binding of factor H to outer membrane proteins. *FEMS Microbiol. Lett.* **301**, 224–231 (2009).
15. Smani, Y., McConnell, M. J. & Pachón, J. Role of fibronectin in the adhesion of *Acinetobacter baumannii* to host cells. *PloS one* **7**, e33073 (2012).
16. Mortensen, B. L. & Skaar, E. P. Host–microbe interactions that shape the pathogenesis of A cinetobacter baumannii infection. *Cell. Microbiol.* **14**, 1336–1344 (2012).
17. Choi, C. H. et al. Outer membrane protein 38 of *Acinetobacter baumannii* localizes to the mitochondria and induces apoptosis of epithelial cells. *Cell. Microbiol.* **7**, 1127–1138 (2005).
18. Tiku, V. et al. Outer membrane vesicles containing OmpA induce mitochondrial fragmentation to promote pathogenesis of *Acinetobacter baumannii*. *Sci. Rep.* **11**, 618 (2021).
19. Jin, J. S. et al. *Acinetobacter baumannii* secretes cytotoxic outer membrane protein A via outer membrane vesicles. *PloS one* **6**, e17027 (2011).
20. Choi, C. H. et al. *Acinetobacter baumannii* outer membrane protein A targets the nucleus and induces cytotoxicity. *Cell. Microbiol.* **10**, 309–319 (2008).
21. Viale, A. M. & Evans, B. A. Microevolution in the major outer membrane protein OmpA of *Acinetobacter baumannii*. *Microb. genomics* **6**, e000381 (2020).
22. Limansky, A. S., Mussi, M. A. & Viale, A. M. Loss of a 29-kilodalton outer membrane protein in *Acinetobacter baumannii* is associated with imipenem resistance. *J. Clin. Microbiol.* **40**, 4776–4778 (2002).
23. Mussi, M. A., Limansky, A. S. & Viale, A. M. Acquisition of resistance to carbapenems in multidrug-resistant clinical strains of *Acinetobacter baumannii*: natural insertional inactivation of a gene encoding a

member of a novel family of β-barrel outer membrane proteins. *Antimicrob. Agents Chemother.* **49**, 1432–1440 (2005).
24. Kuo, H.-Y. et al. Functional characterization of *Acinetobacter baumannii* lacking the RNA chaperone Hfq. *Front. Microbiol.* **8**, 2068 (2017).
25. Uppalapati, S. R., Sett, A. & Pathania, R. The outer membrane proteins OmpA, CarO, and OprD of *Acinetobacter baumannii* confer a two-pronged defense in facilitating its success as a potent human pathogen. *Front. Microbiol.* **11**, 589234 (2020).
26. Smani, Y. et al. Platelet-activating factor receptor initiates contact of *Acinetobacter baumannii* expressing phosphorylcholine with host cells. *J. Biol. Chem.* **287**, 26901–26910 (2012).
27. Hua, M. et al. The novel outer membrane protein from OprD/Occ family is associated with hypervirulence of carbapenem resistant *Acinetobacter baumannii* ST2/KL22. *Virulence* **12**, 1–11 (2021).
28. Smani, Y., Dominguez-Herrera, J. & Pachón, J. Association of the outer membrane protein Omp33 with fitness and virulence of *Acinetobacter baumannii*. *J. Infect. Dis.* **208**, 1561–1570 (2013).
29. Han, L. et al. An outer membrane protein YiaD contributes to adaptive resistance of meropenem in *Acinetobacter baumannii*. *Microbiol. Spectr.* **10**, e00173–00122 (2022).
30. Na, S. H., Jeon, H., Oh, M. H., Kim, Y. J. & Lee, J. C. Screening of small molecules attenuating biofilm formation of *Acinetobacter baumannii* by inhibition of ompA promoter activity. *J. Microbiol.* **59**, 871–878 (2021).
31. Sánchez-Encinales, V. et al. Overproduction of outer membrane protein A by *Acinetobacter baumannii* as a risk factor for nosocomial pneumonia, bacteremia, and mortality rate increase. *J. Infect. Dis.* **215**, 966–974 (2017).
32. Zeighami, H., Valadkhani, F., Shapouri, R., Samadi, E. & Haghi, F. Virulence characteristics of multidrug resistant biofilm forming *Acinetobacter baumannii* isolated from intensive care unit patients. *BMC Infect. Dis.* **19**, 1–9 (2019).
33. Gallagher, L. A. et al. Resources for genetic and genomic analysis of emerging pathogen *Acinetobacter baumannii*. *J. Bacteriol.* **197**, 2027–2035 (2015).
34. Auer, G. K. et al. Mechanical genomics identifies diverse modulators of bacterial cell stiffness. *Cell Syst.* **2**, 402–411 (2016).
35. Trivedi, R. R. et al. Mechanical genomic studies reveal the role of D-alanine metabolism in Pseudomonas aeruginosa cell stiffness. *MBio* **9**, e01340–01318 (2018).
36. Krasowska, A. & Sigler, K. How microorganisms use hydrophobicity and what does this mean for human needs? *Front. Cell. Infect. Microbiol.* **4**, 112 (2014).
37. Lin, L., Rosenberg, M., Taylor, K. & Doyle, R. Kinetic analysis of ammonium sulfate dependent aggregation of bacteria. *Colloids Surf. B Biointerfaces* **5**, 127–134 (1995).
38. Skerniškytė, J. et al. Surface-related features and virulence among *Acinetobacter baumannii* clinical isolates belonging to international clones I and II. *Front. Microbiol.* **9**, 3116 (2019).
39. Pompilio, A. et al. Gram-negative bacteria holding together in a biofilm: the *Acinetobacter baumannii* way. *Microorganisms* **9**, 1353 (2021).
40. Blaschke, U., Skiebe, E. & Wilharm, G. Novel genes required for surface-associated motility in *Acinetobacter baumannii*. *Curr. Microbiol.* **78**, 1509–1528 (2021).
41. Wand, M. E., Bock, L. J., Turton, J. F., Nugent, P. G. & Sutton, J. M. *Acinetobacter baumannii* virulence is enhanced in Galleria mellonella following biofilm adaptation. *J. Med. Microbiol.* **61**, 470–477 (2012).
42. Zhang, L. et al. CarO promotes adhesion and colonization of *Acinetobacter baumannii* through inhibiting NF-κB pathways. *Int J. Clin. Exp. Med* **12**, 2518–2524 (2019).
43. Auer, G. K. & Weibel, D. B. Bacterial cell mechanics. *Biochemistry* **56**, 3710–3724 (2017).
44. Sun, J., Rutherford, S. T., Silhavy, T. J. & Huang, K. C. Physical properties of the bacterial outer membrane. *Nat. Rev. Microbiol.* **20**, 236–248 (2022).
45. Cao, P. & Wall, D. The fluidity of the bacterial outer membrane is species specific: bacterial lifestyles and the emergence of a fluid outer membrane. *BioEssays* **42**, 1900246 (2020).
46. Rojas, E. R. et al. The outer membrane is an essential load-bearing element in gram-negative bacteria. *Nature* **559**, 617–621 (2018).
47. Egan, A. J. Bacterial outer membrane constriction. *Mol. Microbiol.* **107**, 676–687 (2018).
48. Clavel, T., Germon, P., Vianney, A., Portalier, R. & Lazzaroni, J. C. TolB protein of *Escherichia coli* K-12 interacts with the outer membrane peptidoglycan-associated proteins Pal, Lpp and OmpA. *Mol. Microbiol.* **29**, 359–367 (1998).
49. Lazzaroni, J. C., Germon, P., Ray, M.-C. & Vianney, A. The Tol proteins of *Escherichia coli* and their involvement in the uptake of biomolecules and outer membrane stability. *FEMS Microbiol. Lett.* **177**, 191–197 (1999).
50. Cascales, E., Bernadac, A., Gavioli, M., Lazzaroni, J.-C. & Lloubes, R. Pal lipoprotein of *Escherichia coli* plays a major role in outer membrane integrity. *J. Bacteriol.* **184**, 754–759 (2002).
51. Li, Q. et al. The role of TolA, TolB, and TolR in cell morphology, OMVs production, and virulence of Salmonella Choleraesuis. *AMB Express* **12**, 1–12 (2022).
52. Aono, R., Tsukagoshi, N. & Yamamoto, M. Involvement of outer membrane protein TolC, a possible member of the mar-sox regulon, in maintenance and improvement of organic solvent tolerance of *Escherichia coli* K-12. *J. Bacteriol.* **180**, 938–944 (1998).
53. Tattawasart, U., Maillard, J.-Y., Furr, J. & Russell, A. Outer membrane changes in Pseudomonas stutzeri resistant to chlorhexidine diacetate and cetylpyridinium chloride. *Int. J. Antimicrob. Agents* **16**, 233–238 (2000).
54. Choi, U. & Lee, C.-R. Distinct roles of outer membrane porins in antibiotic resistance and membrane integrity in *Escherichia coli*. *Front. Microbiol.* **10**, 953 (2019).
55. Sato, Y., Unno, Y., Kawakami, S., Ubagai, T. & Ono, Y. Virulence characteristics of *Acinetobacter baumannii* clinical isolates vary with the expression levels of omp s. *J. Med. Microbiol.* **66**, 203–212 (2017).
56. Grinter, R. et al. BonA from *Acinetobacter baumannii* forms a divisome-localized decamer that supports outer envelope function. *Mbio* **12**, e01480–01421 (2021).
57. Roy, R., You, R.-I., Lin, M.-D. & Lin, N.-T. Mutation of the carboxy-terminal processing protease in *Acinetobacter baumannii* affects motility, leads to loss of membrane integrity, and reduces virulence. *Pathogens* **9**, 322 (2020).
58. Furuhata, K., Kato, Y., Goto, K., Hara, M. & Fukuyama, M. Diversity of heterotrophic bacteria isolated from biofilm samples and cell surface hydrophobicity. *J. Gen. Appl. Microbiol.* **55**, 69–74 (2009).
59. Guo, T. et al. Correlation between antibiotic resistance and serum resistance in *Acinetobacter baumannii*. *Int J. Clin. Exp. Med* **12**, 9804–9814 (2019).
60. Sanchez-Larrayoz, A. F. et al. Complexity of complement resistance factors expressed by *Acinetobacter baumannii* needed for survival in human serum. *J. Immunol.* **199**, 2803–2814 (2017).
61. Vogt, J. & Schulz, G. E. The structure of the outer membrane protein OmpX from *Escherichia coli* reveals possible mechanisms of virulence. *Structure* **7**, 1301–1309 (1999).
62. Heffernan, E. J. et al. Specificity of the complement resistance and cell association phenotypes encoded by the outer membrane protein genes rck from Salmonella typhimurium and ail from *Yersinia enterocolitica*. *Infect. Immun.* **62**, 5183–5186 (1994).
63. Rolhion, N. & Darfeuille-Michaud, A. Adherent-invasive *Escherichia coli* in inflammatory bowel disease. *Inflamm. Bowel Dis.* **13**, 1277–1283 (2007).

64. Liu, Y.-F. et al. Loss of outer membrane protein C in *Escherichia coli* contributes to both antibiotic resistance and escaping antibody-dependent bactericidal activity. *Infect. Immun.* **80**, 1815–1822 (2012).
65. Hejair, H. M. et al. Functional role of ompF and ompC porins in pathogenesis of avian pathogenic *Escherichia coli*. *Microb. Pathog.* **107**, 29–37 (2017).
66. Hunger, M., Schmucker, R., Kishan, V. & Hillen, W. Analysis and nucleotide sequence of an origin of an origin of DNA replication in *Acinetobacter calcoaceticus* and its use for *Escherichia coli* shuttle plasmids. *Gene* **87**, 45–51 (1990).
67. Scribano, D. et al. Insights into the Periplasmic Proteins of *Acinetobacter baumannii* AB5075 and the Impact of Imipenem Exposure: A Proteomic Approach. *Int J Mol Sci.* **20**, 3451 (2019).
68. Clemmer, K. M., Bonomo, R. A. & Rather, P. N. Genetic analysis of surface motility in *Acinetobacter baumannii*. *Microbiology* **157**, 2534 (2011).
69. Ambrosi, C. et al. *Acinetobacter baumannii* virulence traits: a comparative study of a novel sequence type with other Italian endemic international clones. *Front. Microbiol.* **8**, 1977 (2017).
70. Nwanyanwu, C. & Abu, G. Influence of growth media on hydrophobicity of phenol-utilizing bacteria found in petroleum refinery effluent. *Int. Res. J. Biol. Sci.* **2**, 6–11 (2013).
71. Stepanović, S. et al. Quantification of biofilm in microtiter plates: overview of testing conditions and practical recommendations for assessment of biofilm production by staphylococci. *APMIS* **115**, 891–899 (2007).
72. Ambrosi, C. et al. *Acinetobacter baumannii* targets human carcinoembryonic antigen-related cell adhesion molecules (CEACAMs) for invasion of pneumocytes. *MSYSTEMS* **5**, e00604–e00620 (2020).
73. Esposito, A. et al. Evolution of *Stenotrophomonas maltophilia* in cystic fibrosis lung over chronic infection: a genomic and phenotypic population study. *Front. Microbiol.* **8**, 1590 (2017).
74. Sansone, L. et al. Nicotine in combination with SARS-CoV-2 affects cells viability, inflammatory response and ultrastructural integrity. *Int. J. Mol. Sci.* **23**, 9488 (2022).
75. Belli, M. et al. Oxygen concentration alters mitochondrial structure and function in in vitro fertilized preimplantation mouse embryos. *Hum. Reprod.* **34**, 601–611 (2019).

Acknowledgements

The authors want to acknowledge support for this project from the Dani Di Giò Foundation-Onlus, Rome, Italy. A special thanks to Raffaele D'Errico, Tamara Del Citto, Alessia Bressan, and Astri D. Tagueha for their technical assistance. This work was supported by funding from the Italian Ministry of Health [Ricerca corrente] IRCCS San Raffaele Roma to C.A. and from Dani Di Giò Foundation-Onlus, Rome, Italy to D.S. and C.A. Salary of D.S. and M.S. were supported by POR Lazio FSE 2014–2020 and Sapienza Ateneo funding and by the Italian Ministry of Health (starting grant SG-2018-12365432), respectively. This work was also supported by Sapienza Ateneo funding (RP12218162DFBF0A) to C.Z. and C. A.

Author contributions

Conceptualization, C.A., D.S. Data curation: C.A. Methodology: C.A., E.C., G.D.B., A.P., M.C., L.S., and M.B. Formal analysis: C.A., D.S., M.S., E.C., G.D.B., A.P., M.C., L.S., and M.B. Resources: C.A., D.S., E.C., G.D.B., A.P., C.Z., M.B., and A.T.P. Writing—original draft preparation: C.A. Writing—review and editing: C.A., D.S., M.S., G.D.B., A.P., and A.T.P. Funding acquisition: C.A., D.S., C.Z., and A.T.P. All authors have read and agreed to the published version of the manuscript.

Competing interests

The authors declare no competing interests.

Additional information

Supplementary information The online version contains supplementary material available at https://doi.org/10.1038/s42003-024-06645-0.

Correspondence and requests for materials should be addressed to Cecilia Ambrosi.

Peer review information *Communications Biology* thanks Benjamin Evans, Ivan Dikic, and the other, anonymous, reviewer for their contribution to the peer review of this work. Primary handling editor: Tobias Goris.